Variational approach to spatial optical solitons in bulk cubic-quintic media stabilized by self-induced multiphoton ionization

C. P. Jisha* and V. C. Kuriakose†
Department of Physics, Cochin University of Science and Technology, Cochin 682022, India

K. Porsezian‡
Department of Physics, Pondicherry University, Pondicherry 605014, India
(Received 30 September 2004; published 25 May 2005)

Propagation of an optical high-power cylindrically symmetric beam in a material characterized by cubic-quintic nonlinearity is studied both analytically and numerically. In this case we have to consider the self-defocusing effect caused by the presence of free electrons produced due to plasma formation. The variational method is used to study the system analytically. The finite-difference beam propagation method is used for the numerical analysis. Stable (2+1)D spatial solitons are observed. The analytical results are found to be in very good agreement with the numerical results.

DOI: 10.1103/PhysRevE.71.056615 PACS number(s): 42.65.Tg

I. INTRODUCTION

A spatial soliton results from the balance between linear diffraction and nonlinear self-focusing, usually with a Kerr-type ultrafast nonlinearity. This effect was discovered in 1964 [1]. It was Askaryan in 1962 [2] who first suggested the idea that an optical beam can induce a waveguide and guide itself in it. A light beam traveling either in vacuum or in a medium always broadens because of the light's natural wave property of diffraction. But if the beam is shone into a bulk nonlinear material, such as silica glass, it changes the material's refractive index. The consequent variation of the velocity of light across the beam's wave front focuses the beam as if it were passing through a lens. The earliest experimental observation of the self-focusing of optical beams was in 1964 [3]. If the beam's diffraction can be compensated by beam's self-focusing, we get the so-called spatial solitons. The perfect balance between diffraction and self-focusing that exists in spatial solitons has been found to occur in one and two transverse dimensions, and the solitons are named (1+1)D or (2+1)D accordingly. These spatial solitons have been found to occur in a variety of materials like Kerr materials, photorefractive materials, liquid crystals, etc. Recently, Peccianti *et al.* [4] set up an experiment to demonstrate all-optical switching and logic gate blocks using spatial solitons in liquid crystals.

The (1+1)D spatial solitons, a continuous wave beam linearly confined in one transverse dimension and self-guided in the other transverse dimension, are stable to perturbations and have been observed experimentally. A (2+1)D soliton that is self-guided in both transverse dimensions is not stable with a Kerr-type nonlinearity. Additional mechanisms such as index saturation or inclusion of higher-order nonlinearity helps to stabilize the propagation of such beams.

A simple model for the stable propagation of (2+1)D solitons may be based on cubic-quintic nonlinearity [5,6]. This model has attracted considerable attention. It has been shown that the cubic-quintic nonlinearity correctly describes the dielectric response of the polydiacetylene *p*-toluene sulfonate (PTS) crystal [7]. This type of nonlinear response is known for semiconductor-doped glasses and various π-conjugated polymers [8–10]. In these types of materials the refractive index n is of the form

$$n = n_0 + n_2 I + n_4 I^2, \tag{1}$$

where I is the beam intensity, n_0 is the linear refractive index, and n_2 and n_4 are nonlinear coefficients with $n_2 > 0$ and $n_4 < 0$; i.e., the higher-order nonlinearity is of the saturating kind. The propagation of spatial solitons in a PTS like medium has been studied by various groups [11–13]

Now, if we are using a high-power laser beam, we have to consider the phenomenon of plasma generation through multiphoton absorption. For an extreme high-power laser pulse of the order of 10 TW relativistic self-channeling in an underdense plasma has been predicted and experimentally observed over a plasma length of 3 mm. In this regime nearly all molecules of the medium are ionized and relativistic self-focusing develops from an increase of electron inertia under the influence of the intense electromagnetic wave. When such pulses are propagated through air, they can propagate over considerable distances because of the formation of filaments after the plasma has been generated through multiphoton ionization of air [14]. The dispersive effects are less important in this case. The main mechanism behind the filament formation is related to a dynamic balance between the Kerr self-focusing and the defocusing induced by the plasma [15].

The idea of controlling light with light by taking advantages of nonlinear optical effects is a topic of interest to many researchers and scientists. The fundamental benefit is in the possibility of avoiding any optoelectronic conversion process and hence increasing the device speed and efficiency. It is in this scenario, the self-guided beams called "spatial

*Electronic address: jisha@cusat.ac.in
†Electronic address: vck@cusat.ac.in
‡Electronic address: ponzsol@yahoo.com

solitons" find importance. The areas of application include all-optical switching devices [16], optical computing, all-optical polarization modulators [17], logic gates, etc. The prospect of forming all-optical switches and logic gates presents promise for generations of novel optical interconnects for computing and communications.

In the present work, we have studied the propagation of an optical high-power beam through a PTS-like medium. In this high-energy regime, we have to consider the phenomenon of plasma generation through multiphoton absorption [18]. Multiphoton absorption is a nonlinear process, in contrast with the one-photon absorption process. It has a self-defocusing effect on the material. The counteracting self-defocusing effect of both photoionized free electrons and the quintic nonlinearity restricts the unbounded growth of the Kerr nonlinearity. The study of spatial solitons in a bulk Kerr medium with multiphoton ionization has been carried out by Henz and Herrmann [19]. Couairon [20] has studied the dynamics of light filaments formed when a femtosecond laser pulse propagates in air, taking into consideration the plasma generated using photoionization.

The refractive index now takes the form $n=n_0+n_2I+n_4I^2-N_e/2n_0N_{cr}$, where N_e is the number density of free electrons and N_{cr} is the critical plasma density.

The beam evolution is studied using the cubic-quintic nonlinear Schrödinger equation with the effect of multiphoton ionization. We analyzed the problem using both numerical and analytical methods.

We used the variational method [21] with a Gaussian ansatz for the analytical analysis. Approximate solutions can be found using this method. The solutions obtained using the variational method were used as initial conditions for the direct integration to obtain a numerical solution. The finite-difference beam propagation method (FD-BPM) was used for the numerical analysis [22].

II. ANALYTICAL ANALYSIS USING THE VARIATIONAL METHOD

An electric field $E(r,t)$ in a dielectric medium satisfies Maxwell's equation in the form

$$\nabla^2 E - \frac{1}{c^2}\frac{\partial^2 D}{\partial t^2} = \nabla(\nabla\cdot\mathbf{E}), \tag{2}$$

where $D=\epsilon E$ is the displacement vector in the dielectric medium, with ϵ being the dielectric constant relative to vacuum and it is approximately equal to n^2, n being the refractive index. For a medium characterized by cubic nonlinearity, D can be written as $D=[n_0(\omega)+n_2(\omega)|E|^2]^2E$ where, $E=\frac{1}{2}[A(r,t)\exp i(wt-kz)+\text{c.c.}]$. Using this we can reduce Maxwell's equation to

$$2ik\frac{\partial A}{\partial z} + \nabla^2 A + 2kk_0 n_2|A|^2A = 0 \tag{3}$$

for a cubic medium where $k=\omega/c$, $k_0=n_0k$, and A is the amplitude of the beam. This is the cubic nonlinear Schrödinger equation.

There are many materials which show quintic nonlinear effect in addition to the cubic one. In this case Maxwell's equation can be simplified to obtain the cubic-quintic nonlinear Schrödinger equation. Hence the dynamics of the amplitude A of a laser beam in a PTS-like medium is governed by a cubic-quintic nonlinear Schrödinger equation of the form

$$2ik\frac{\partial A}{\partial z} + \nabla^2 A + 2kk_0 n_2|A|^2A + 2kk_0 n_4|A|^4A = 0. \tag{4}$$

Since we are using a very-high-power laser beam, we have to consider the effect of multiphoton ionization as well. The reduced Maxwell's equation for the slowly varying amplitude A now takes the form

$$i2k\frac{\partial A}{\partial z} + \nabla^2 A + 2kk_0 n_2|A|^2A + 2kk_0 n_4|A|^4A - \rho aA\int_{-\infty}^{\eta}|A(t')|^{2N}dt' = 0, \tag{5}$$

where N is the number of quanta necessary to ionize the molecules, $\eta=t-z/v$ is the time of the moving frame of the pulse maximum, and ρ and a are constants.

Here, we are considering the propagation of the beam along the z direction and variation along the radial direction. So we will use cylindrical coordinates for our analysis. Hence Eq. (5) takes the form

$$i2k\frac{\partial A}{\partial z} = -\frac{1}{r}\frac{\partial}{\partial r}\left(r\frac{\partial A}{\partial r}\right) + 2k\lambda_1|A|^2A + 2k\lambda_2|A|^4A + \rho aA\int_{-\infty}^{\eta}|A(t')|^{2N}dt. \tag{6}$$

Here $\lambda_1=-k_0n_2$ and $\lambda_2=-k_0n_4$

The time dependence of the beam is taken into account by the ansatz $A(z,r,\eta)=B(z,r)T(\eta)$. $T(\eta)$ is the normalized input shape.

Equation (6) can be obtained from the Lagrangian

$$L = i\frac{r}{2}\left(B\frac{\partial B^*}{\partial z} - B^*\frac{\partial B}{\partial z}\right)T + \frac{r}{2k}\frac{\partial B}{\partial r}\frac{\partial B^*}{\partial r}T + r\frac{\lambda_1}{2}|B|^4T^3 + r\frac{\lambda_2}{3}|B|^6T^4 + r\frac{\rho a}{2k}\frac{|B|^{2N+2}}{N+1}Tg(\eta), \tag{7}$$

where

$$g(\eta) = \int_{-\infty}^{\eta} T^{2N}dt.$$

For a solution of this problem, let us assume a trial solution of the form

$$B(z,r) = C(z)\exp\left[-\frac{r^2}{2w(z)^2} + ib(z)r^2\right], \tag{8}$$

where $C(z)$ is the maximum amplitude, $b(z)$ is the curvature parameter, and $w(z)$ is the beam radius. Ideally, the trial function should include a possibility to model the dynamically varying radial shape function of the beam. But that will make the variational analysis more complicated.

The reduced Lagrangian is then given by

$$\langle L\rangle = \int_0^\infty L r dr, \tag{9}$$

$$\langle L\rangle = i\frac{T}{2}\left(C\frac{\partial C^*}{\partial z} - C^*\frac{\partial C}{\partial z}\right)w^3\frac{\sqrt{\pi}}{4} + b_z|C|^2Tw^5\frac{\sqrt{\pi}}{8} + \frac{|C|^2T}{2k}\left\{\frac{1}{w^4} + 4b^2\right\}w^5\frac{\sqrt{\pi}}{8} + \frac{\lambda_1}{2}|C|^4T^3w^3\frac{\sqrt{\pi}}{8\sqrt{2}} + \frac{\lambda_2}{3}|C|^6T^4w^3\frac{\sqrt{\pi}}{12\sqrt{3}} + \frac{\rho a}{2k}\frac{|C|^{2N+2}}{(N+1)^{5/2}}Tg(\eta)w^3\frac{\sqrt{\pi}}{4}. \tag{10}$$

Now we can find the variation of $\langle L\rangle$ with respect to the various Gaussian parameters $C(z)$, $C(z)^*$, $w(z)$, and $b(z)$:

$$C\frac{\partial\langle L\rangle}{\partial C} = i\frac{T}{2}CC_z^*w^3 + b_z|C|^2T\frac{w^5}{2} + \frac{|C|^2T}{2k}\left\{\frac{1}{w^4} + 4b^2\right\}\frac{w^5}{2} + \frac{\lambda_1}{2\sqrt{2}}|C|^4T^3w^3 + \frac{\lambda_2}{3\sqrt{3}}|C|^6T^4w^3 + \frac{\rho a}{2k}\frac{|C|^{2N+2}}{(N+1)^{5/2}}Tg(\eta)w^3 \tag{11}$$

and

$$C^*\frac{\partial\langle L\rangle}{\partial C^*} = -i\frac{T}{2}C^*C_zw^3 + b_z|C|^2T\frac{w^5}{2} + \frac{|C|^2T}{2k}\left\{\frac{1}{w^4} + 4b^2\right\}\frac{w^5}{2} + \frac{\lambda_1}{2\sqrt{2}}|C|^4T^3w^3 + \frac{\lambda_2}{3\sqrt{3}}|C|^6T^4w^3 + \frac{\rho a}{2k}\frac{|C|^{2N+2}}{(N+1)^{5/2}}Tg(\eta)w^3. \tag{12}$$

Subtracting Eq. (12) from Eq. (11), we get

$$\frac{iT}{2}CC_z^*w^3 + \frac{iT}{2}C^*C_zw^3 = 0$$

$$\Rightarrow |C|^2 = y \text{ (a constant)}$$

$$\Rightarrow w(0)^2|C(0)|^2 = w(z)^2|C(z)|^2 = E_0. \tag{13}$$

Adding Eqs. (11) and (12) we obtain

$$i(CC_z^* - C^*C_z) = -2b_z|C|^2w^2 - \frac{2|C|^2}{2k}\left\{\frac{1}{w^4} + 4b^2\right\}w^2 - \frac{2\lambda_1}{\sqrt{2}}|C|^4T^2 - \frac{4\lambda_2}{3\sqrt{3}}|C|^6T^3 + \frac{4\rho a}{2k}\frac{g(\eta)|C|^{2N+2}}{(N+1)^{5/2}}. \tag{14}$$

Now, the variation of $\langle L\rangle$ with respect to $w(z)$ and b gives

$$\frac{\partial\langle L\rangle}{\partial w} = \frac{3}{2}iT(CC_z^* - C^*C_z) + 5b_z|C|^2T\frac{w^4}{2} + \frac{|C|^2T}{4k} + 10|C|^2Tb^2\frac{w^4}{2k} + \frac{3\lambda_1}{4\sqrt{2}}|C|^4T^3w^2 + \frac{\lambda_2}{3\sqrt{3}}|C|^6T^4w^2 + \frac{3\rho a}{2k}\frac{|C|^{2N+2}}{(N+1)^{5/2}}Tg(\eta)w^2 \tag{15}$$

and

$$\frac{\partial\langle L\rangle}{\partial b} = 0 \Rightarrow \frac{d}{dz}(w^5|C|^2) = \frac{6b}{k}|C|^2w^5. \tag{16}$$

From this and considering the fact that $w^2|C|^2$ is a constant, we can write

$$\frac{dw}{dz} = \frac{4bw}{2k}. \tag{17}$$

This implies

$$b(z) = \frac{k}{2}\frac{d\ln w}{dz}. \tag{18}$$

Comparing Eqs. (14) and (15) we obtain

$$b_zw^2 + \frac{5}{2kw^2} + \frac{4b^2w^2}{2k} + \frac{9\lambda_1}{2\sqrt{2}}|C|^2T^2 + \frac{10\lambda_2}{3\sqrt{3}}|C|^4T^3 + \frac{6(2N+1)\rho a}{2k(N+1)}\frac{|C|^{2N}}{(N+1)^{5/2}}g(\eta) = 0. \tag{19}$$

Now, combining Eq. (19) with the derivative form of Eq. (17), we obtain

$$\frac{d^2w}{dz^2} = -\frac{20}{(2k)^2w^3} - \frac{36\lambda_1T^2E_0}{4k\sqrt{2}w^3} - \frac{40\lambda_2T^3E_0^2}{6k\sqrt{3}w^5} - \frac{24(2N+1)\rho a g(\eta)E_0^N}{(2k)^2(N+1)^{5/2}w^{2N+1}}. \tag{20}$$

Here $|C|^2$ has been eliminated by using the fact that $w^2|C|^2 = E_0$.

On integrating the above equation, we get an equation for the variation of $w(z)$ as

$$\frac{1}{2}\left(\frac{dw}{dz}\right)^2 + \Pi(w) = 0. \tag{21}$$

This is analogous to the equation of a particle moving in a potential well. The potential $\Pi(w)$ is given by

$$\Pi(w) = -\frac{10}{(2k)^2w^2} - \frac{18\lambda_1T^2E_0}{4k\sqrt{2}w^2} - \frac{10\lambda_2T^3E_0^2}{6k\sqrt{3}w^4} - \frac{24(2N+1)\rho a g(\eta)E_0^N}{2N(2k)^2(N+1)^{5/2}w^{2N}} + c. \tag{22}$$

The phase $\phi(z)$ of $C(z)$ **(**$C(z) = |C(z)|\exp[i\phi(z)]$**)** is obtained from Eq. (14), and also using Eq. (19) we find

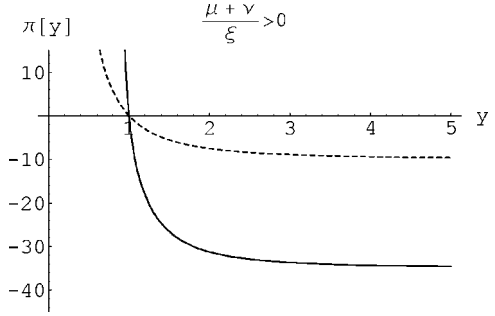

FIG. 1. Qualitative plot of the potential function $\Pi(y)$ when all the nonlinearities are of defocusing nature $[(\mu+\nu)/\xi>0]$. The dotted line represents the linear case.

$$\frac{d\phi}{dz} = \frac{4}{2kw^2} + \frac{7\lambda_1}{2\sqrt{2}}|C|^2T^2 + \frac{8\lambda_2}{3\sqrt{3}}|C|^4T^3 + \frac{2(7N+4)\rho a}{(N+1)2k}\frac{g(\eta|C|^{2N})}{(N+1)^{5/2}}. \tag{23}$$

Introducing $w(z)/w_0 = y(z)$, Eq. (21) becomes

$$\frac{1}{2}\left(\frac{dy}{dz}\right)^2 + \Pi(y) = 0, \tag{24}$$

where

$$\Pi(y) = \frac{\mu}{y^2} + \frac{\nu}{y^4} + \frac{\xi}{y^{2N}} + K,$$

$$\mu = -\frac{10}{4k^2w_0^4} - \frac{18\lambda_1T^2E_0}{4k\sqrt{2}w_0^4},$$

$$\nu = -\frac{10\lambda_2T^3E_0^2}{6k\sqrt{3}w_0^6},$$

$$\xi = -\frac{24(2N+1)\rho a g(\eta)E_0^N}{2N(2k)^2(N+1)^{5/2}w_0^{2N+2}},$$

$$K = \frac{c}{w_0^2}. \tag{25}$$

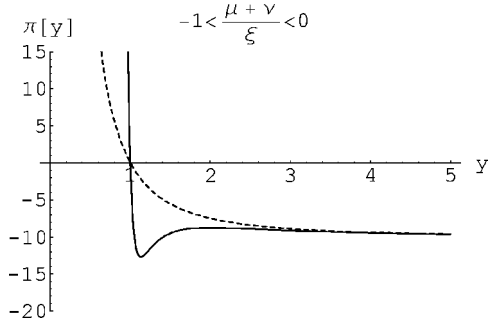

FIG. 2. Qualitative plot of the potential function $\Pi(y)$ when third-order nonlinearity is of focusing nature and all other nonlinearities are of defocusing nature (weak fifth order) $[-1<(\mu+\nu)/\xi<0]$. The dotted line represents the linear case.

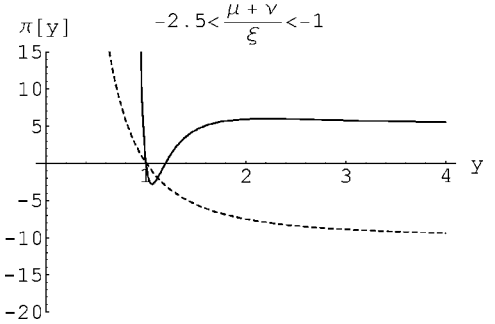

FIG. 3. Qualitative plot of the potential function $\Pi(y)$ when third-order nonlinearity is of focusing nature and all other nonlinearities are of defocusing nature (strong fifth order) $[-2.5<(\mu+\nu)/\xi<-1]$. The dotted line represents the linear case.

Now, let us assume that the beam at $z=0$ has $w(0)=w_0$ and $[dw(z)/dz]_{z=0}=0$. This gives $K=-(\mu+\nu+\xi)$.

Depending on the values of μ, ν, and ξ we can identify four different regimes.

(1) $(\mu+\nu)/\xi>0$. This condition implies defocusing due to both third- and fifth-order nonlinearities as well as the nonlinearity due to the multiphoton effect. We can clearly see from Fig. 1 that the beam diffracts faster than in the purely linear case.

(2) $-1<(\mu+\nu)/\xi<0$. This condition implies focusing due to the third-order nonlinearity and defocusing due to a weak fifth-order nonlinearity. The multiphoton effect is also of defocusing nature. We can see (Fig. 2) that the nonlinearity is trying to focus the beam.

(3) $-2.5<(\mu+\nu)/\xi<-1$. In this case the third-order nonlinearity is of the focusing case and there is a strong fifth-order nonlinearity. A potential well has been created. The spreading of the beam is stopped at the zeros of the potential function (Fig. 3).

(4) $(\mu+\nu)/\xi=-2.5$. This is the limit case. The potential well has degenerated into a single point. The diffraction of the beam is exactly compensated by the focusing effect of the nonlinearity and beam propagates without any change in its shape (Fig. 4). The collapse of the beam has been arrested and we get a stable $(2+1)$D spatial soliton which propagates

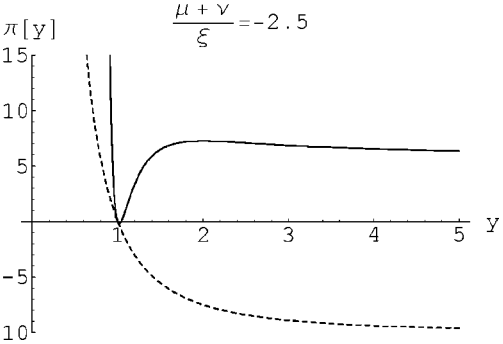

FIG. 4. Qualitative plot of the potential function $\Pi(y)$ when focusing due to the third-order nonlinearity is completely balanced by the defocusing due to the fifth-order nonlinearity and multiphoton ionization $[(\mu+\nu)/\xi=-2.5]$. This is the limit case. The dotted line represents the linear case.

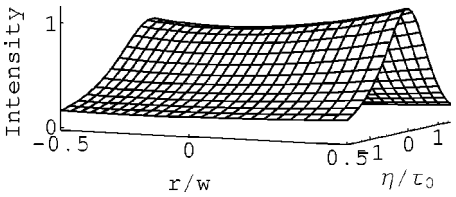

FIG. 5. Three-dimensional plot of the normalized soliton intensity vs the time η and the radial variable r.

through the medium without any shape change.

A three-dimensional plot of the normalized soliton intensity vs the time η and the radial variable r is plotted (Fig. 5).

III. NUMERICAL ANALYSIS

Equation (5) is numerically studied using the FD-BPM. It is a cylindrical partial differential equation that can be "integrated" forward in z by a number of standard techniques. In this approach, the field in the transverse plane is represented only at discrete points on a grid and at discrete planes along the propagation direction z. Given the field at one z plane, we can find the field at the next z plane. This is then repeated to determine the field throughout the structure.

Let Ψ_i^{s+1} denote the field at transverse grid point i and longitudinal plane s_i, and assume that the grid points and planes are equally spaced by Δr and Δz apart, respectively. The radial and longitudinal dimensions are discretized by the values r_i and z_s according to the relations

$$r_i = i\Delta r \quad \text{and} \quad z_s = s\Delta z$$

We get a tridiagonal matrix of the form

$$-c_1\Psi_{i+1}^{s+1} + d\Psi_i^{s+1} - c_3\Psi_{i-1}^{s+1} = c_1\Psi_{i+1}^{s} + c_2\Psi_i^{s} + c_3\Psi_{i-1}^{s}.$$

This can be easily solved using the Thomas algorithm [23]. Once the field at s is known, we can determine the field at $s+1$ and so on.

We integrated Eq. (5) using the result obtained from the variational analysis as initial condition. The numerical parameters of the simulation has been chosen so as to fit the usual experimental configurations. Here, we have chosen $n_0=1.6755$, $n_2=2.2\times10^{-12}$ cm^2/W and $n_4=-8\times10^{-22}$ cm^4/W^2 which are the nonlinear coefficients of PTS at wavelength 1600 nm [24]. Similarly, for AlGaAs, with $n_0=3$, $n_2=1.5\times10^{-13}$ cm^2/W, $n_4=-5\times10^{-23}$ cm^4/W^2 at wavelength 1550 nm [24]. The beam intensity is chosen as 1.1×10^9 W/m^2. The outcome of these simulations (see Fig. 6) agrees very well with that obtained from the variational approach. The beam propagates without any change in shape.

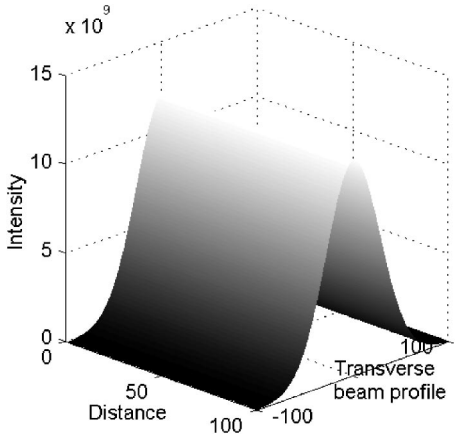

FIG. 6. Numerically computed beam profile after it propagates a distance of 1 mm through the medium. Here intensity is in W/m^2 and distance and transverse beam profile are in micrometers.

IV. RESULTS AND DISCUSSION

In this work we have studied, both analytically and numerically, the propagation of a high-energy laser beam through a PTS like medium characterized by both third- and fifth-order nonlinearities. The energy of the beam considered in the present problem is sufficiently high enough to produce multiphoton ionization. Solutions are obtained using the variational formulation. It is found that multiphoton ionization helps in containing the catastrophic breakdown of the beam and helps in forming stable solitons. We could also show analytically the formation of stable solitons. This solution was taken as the initial condition for the numerical simulation. The soliton is found to propagate without any shape change.

ACKNOWLEDGMENTS

The authors acknowledge UGC, New Delhi for providing computer facility through DSA (Phase II) program. J.C.P. wishes to thank Cochin University of Science and Technology for providing financial assistance. V.C.K. wishes to acknowledge DST, Government of India for financial support in the form of a research grant. K.P wishes to thank DST, CSIR, and UGC (Research Award) for financial help through projects.

[1] R. Y. Chiao, E. Garmire, and C. H. Townes, Phys. Rev. Lett. **13**, 479 (1964).
[2] G. A. Askaryan, Sov. Phys. JETP **15**, 1088 (1962).
[3] M. Hercher, J. Opt. Soc. Am. **54**, 563 (1964).
[4] M. Peccianti, Claudio Conti, and Gaetano Assanto, Appl. Phys. Lett. **81**, 3335 (2002).
[5] Kh. I. Pushkarov, D. I. Pushkarov, and I. V. Tomov, Opt. Quantum Electron. **11**, 471 (1979).
[6] S. Cowan, R. H. Enns, S. S. Ranganekar, and S. S. Sanghera, Can. J. Phys. **64**, 311 (1986).
[7] B. L. Lawence, M. Cha, J. U. Kang, W. Torruellas, G. Stegeman, G. Baker, J. Meth, and S. Etemad, Electron. Lett. **30**, 889 (1994).
[8] P. Roussignol, D. Ricard, J. Lukasik, and C. Flytzanis, J. Opt.

Soc. Am. B **4**, 5 (1987).
[9] L. H. Acioli, A. S. L. Gomes, J. M. Hickmann, and C. B. De Araujo, Appl. Phys. Lett. **56**, 2279 (1990).
[10] F. Lederer and W. Biehlig, Electron. Lett. **30**, 1871 (1994).
[11] K. Dimitrevski *et al.*, Phys. Lett. A **248**, 369 (1998).
[12] D. Pushkarov and S. Tanev, Opt. Commun. **124**, 354 (1996).
[13] H. Michinel, J. Campo-Taboas, M. L. Quiroga-Teixeiro, J. R. Salgueiro, and R. Garcia-Fernandez, J. Opt. B: Quantum Semiclassical Opt. **3**, 314 (2001).
[14] M. Mlejnek, M. Kolesik, J. V. Moloney, and E. M. Wright, Phys. Rev. Lett. **83**, 2938 (1999).
[15] N. Akozbek, C. M. Bowden, A. Talebpour, and S. L. Chin, Phys. Rev. E **61**, 4540 (2000).
[16] V. Van *et al.*, IEEE J. Quantum Electron. **14**, 74 (2002).
[17] G. Cancellieri, F. Chiaraluce, Ennio Gambi, and Paola Pierleoni, J. Lightwave Technol. **14**, 513 (1996).
[18] Yuri S. Kivshar and Govind P. Agrawal, *Optical Solitons—From Fibers to Phtonic Crystals* (Academic, San Diego, California, 2003).
[19] S. Henz and J. Herrmann, Phys. Rev. E **53**, 4092 (1996).
[20] A. Couairon, Phys. Rev. A **68**, 015801 (2003).
[21] D. Anderson, Phys. Rev. A **27**, 3135 (1983).
[22] R. Scarmozzino, A. Gopinath, R. Pregla, and S. Helfert, IEEE J. Sel. Top. Quantum Electron. **6**, 150 (2000).
[23] A. Gourdin and M. Boumahrat, *Applied Numerical Methods* (Prentice Hall, New Delhi, 1996).
[24] S. Saltiel, S. Tanev, and A. D. Boardman, Opt. Lett. **22**, 148 (1997).